Fabrication and Photovoltaic Characterization of Bio-Sensitized Solar Cells Using Myoglobin-Based Sensitizers

Chih-Wei Chang[1], Chin-Hao Chang[2], Hsueh-Pei Lu[1],
Tung-Kung Wu[2, *], and Eric Wei-Guang Diau[1, *]

[1]*Department of Applied Chemistry and Institute of Molecular Science, and*
[2]*Department of Biological Science and Technology, National Chiao Tung University, Hsinchu 30010, Taiwan*

Myoglobin (Mb), reconstituted zinc protoporphyrin-apomyoglobin (ZnMb), and eosin-modified ZnMb (EoZnMb) were used as photosensitizers to functionalize TiO_2 nanocrystalline films for bio-sensitized solar-cell (BSSC) applications. For the Mb-sensitized SC, the poor cell performance was due to a reduction $Fe(III) \rightarrow Fe(II)$ that produces a photocurrent density of the device smaller than its unsensitized counterpart. The efficiencies of power conversion of both ZnMb and EoZnMb–sensitized SC were enhanced about ten times due to superior charge separation between TiO_2 and the protein, and due to smaller current leakage between TiO_2 and the electrolyte. The cell performances of the BSSC devices are discussed in terms of an equivalent-circuit model.

Keywords:

1. INTRODUCTION

With the ever increasing population of the earth, the demand for energy becomes the most important problem for the next 50 years.[1] Most energy is provided at present by burning fossil fuel, but the extensive usage of fossil fuel produces also a greatly increased concentration of atmospheric CO_2 that causes global warming.[2] A search for a clean and sustainable source of energy free of carbon has therefore become an important issue for scientists. The most obvious source is the sun, which supplies energy about ten thousand times what all mankind consumes currently.[1] Solar photovoltaic cells, capable of directly converting sunlight into electrical power, are the best candidates for a clean and renewable future source of energy. Although a Si-based solar cell has been developed and commercialized for more than 30 years, a most promising photovoltaic cell is a dye-sensitized solar cell (DSSC). The idea of this DSSC was initiated in the early 1970's,[3] but Grätzel and his co-workers achieved a major advance in 1991.[4]

A typical DSSC device comprises a photo-active dye, a mesoporous nanocrystalline semiconductor layer coated on a transparent conducting oxide (TCO) substrate (anode), a liquid electrolyte (I^-/I_3^- in acetonitrile), and a Pt-coated TCO substrate (cathode). Upon excitation, the excited dye molecules inject electrons into the conduction band of the nanocrystalline semiconductor. The electrons are collected by the TCO anode and flow through the outer circuit to the Pt-coated cathode. I_3^- becomes reduced to three I^- by the excess electrons at the cathode, and the three I^- become oxidized back to I_3^- to regenerate the dye molecules at the anode. In a DSSC, molecules of an appropriately chosen dye play an important role in determining the overall cell performance; many dyes such as ruthenium polypyridine complexes,[1, 5] phthalocyanine,[6, 7] xanthenes,[8, 9] and coumarins[10, 11] have hence been tested as potential sensitizers. The greatest efficiency (η) of power conversion, 11%, has been achieved using ruthenium bi-pyridine derivatives,[1, 5] but the toxic and scarce synthetic organic and inorganic dyes might cause problems also in their mass production and environmental impact. For these reasons, seeking natural dye molecules has been an important issue under investigation.
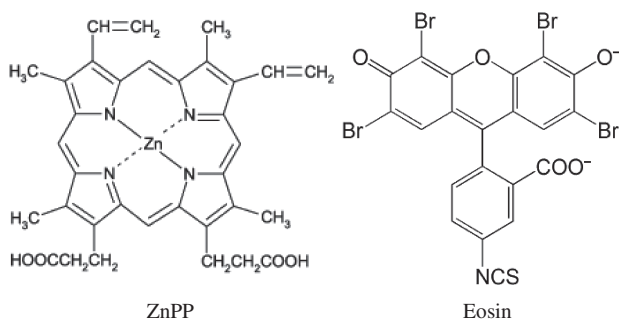
Many biomaterials such as natural dyes extracted from plants,[12] cyanobacteria cells,[13] living whole-cell photo-synthetic micro-organisms[14] and protein with solid-state electronics.[15, 16] have been tested in making bio-sensitized solar cells (BSSC).[17] Tsujimura et al.[18] used the whole cells of *Synechococcus* sp. PCC7942 as a biocatalyst and

*Authors to whom correspondence should be addressed.

2,6-dimethyl-1,4-benzoquinone (DMBQ) as a mediator to produce a photosynthetic bioelectrochemical cell with a photoconversion efficiency ~2% under illumination from a desktop fluorescent lamp. Lam et al.[19] demonstrated a microelectromechanical system (MEMS) photosynthetic electrochemical cell (μPEC) that harnesses the subcellular thylakoid photosystems isolated from spinach cells to convert radiant energy into electricity; the device produced $V_{OC} = 470$ mV and $I_{SC} = 1.1$ μA cm^{-2} with a photoconversion efficiency 0.01%. Lu et al.[20] entrapped the bacterial photosynthetic reaction center (RC) from *Rb. Sphaeroides* strain RS601 on three-dimensional worm-like mesoporous WO$_3$-TiO$_2$ films to develop versatile bio-photoelectric devices; the I_{SC} was detected near 30 μA cm^{-2} with a maximal incident conversion efficiency of photons to current (IPCE) ~11% (about 800 nm). Among those biosensitizers, the most promising are derivatives of metalloporphyrins, of which the porphyrins are integrated with metals of various types.

Metalloporphyrins play an important role in nature. Fe protoporphyrin (heme) is an essential factor for transport and storage of O$_2$ whereas Mg protoporphyrin (MgPP) is a key element in the conversion of radiant energy to chemical energy in photosynthesis. The capability of porphyrins to adsorb visible light in regions 400–450 nm (Soret or B band) and 500–700 nm (Q bands) makes it an effective candidate as a sensitizer.[21–24] Through chemical modification, $\eta \sim 7.1\%$ has been achieved with a DSSC based on Zn porphyrin,[25] but a serious limitation arises from the tendency of the porphyrin to aggregate, which competes with electron injection and yields a decreased overall efficiency of power conversion in the device. In our previous work,[26] employing both steady-state and temporally resolved spectral techniques, we demonstrated that the aggregation of zinc protoporphyrin (ZnPP, structure shown in Chart 1) is successfully suppressed on encapsulation within apomyoglobin (apoMb). According to previous workers,[27–29] the immobilization of proteins on a TiO$_2$ film is achievable through an electrostatic force between the protein and the TiO$_2$ surface so that proteins serve as biosensors.

Eosin is a chromophore of one kind with red fluorescence that is usable to stain cytoplasm, collagen and muscle fibers for examination under a microscope. When redox-proteins are modified with eosin, the redox-protein becomes converted to a light-activated biocatalyst, a 'photoenzyme.'[30] These modified proteins act as a photoenzyme for photoinduced hydrogenation of ethyne to form ethene. The photoelectrochemical behavior of eosin was also investigated on coupling eosin with SnO$_2$/TiO$_2$ films to a DSSC device; the maximum IPCE of this system was reported to be 63% at 525 nm.[31] Eosin might thus also be an effective chromophore to modify proteins in a BSSC so as to improve the efficiency of energy conversion. To extend the region of spectral absorption, eosin-5-isothiocyanate (Eosin, structure shown in Chart 1) was also tested as an auxiliary sensitizer because its absorption spectrum is complementary to that of ZnPP. In this paper, we report the cell performance of BSSC devices using Mb, ZnMb and Eosin-modified ZnMb (EoZnMb) as biosensitizers. Relative to blank TiO$_2$ films, the photocurrent of a Mb-sensitized solar cell decreases significantly, but we found the efficiency of power conversion to be enhanced more than ten times both ZnMb- and EoZnMb-sensitized SC. The modification of Eosin on ZnMb significantly increases the photocurrent; we propose a mechanism.

2. EXPERIMENTAL DETAILS

2.1. Preparation of apoMb

Apomyoglobin was prepared by the modified butanone method of heme extraction.[32] In brief, to extract the heme prosthetic group we dissolved horse-heart myoglobin (100 mg) in PBS buffer (ice-cold, salt-free, 30 mL) and adjusted to pH 2.0 with HCl (0.1 M). The denatured protein solution was treated with ice-cold butanone (an equal volume) and shaken well until a hazy, pale yellow, protein layer separated from the dark brown, heme-containing layer. To remove residual heme from Mb we washed the aqueous phase further with ice-cold butanone (three portions). The resulting aqueous layer was dialyzed twice against dd H$_2$O and then repeatedly against a phosphate buffer solution (10 mM, pH 7.0). The resulting apoMb solution was lyophilized; the solid was preserved at -20 °C until use.

2.2. Reconstitution of Apomyoglobin (apoMb) with ZnPP

The reconstitution of zinc (II) protoporphyrin into apoMb was performed according to the modified method of Hamachi et al.[33–35] The apoMb (4 mg) was dissolved in KPi/DMSO (5 mL, 100 mM, 4:1 v/v) buffer; the pH of the solution was adjusted to 12 on adding NaOH (0.5 M). To the apoMb solution was added dropwise ZnPP (1.6 mg, 1.5 molar equivalent), which was previously dissolved in KPi/pyrimidine solution (500 mL, 1:1). The solution was slowly stirred in an ice bath for 15 min before the pH

Chart 1. Chemical structures of Zinc protoporphyrin (ZnPP) and eosin-5-isothiocyanate (Eosin) molecules.

was adjusted to 6.8. The ZnPP-apoMb mixture was slowly stirred at 4 °C for an additional 6 h. The resulting solution was dialyzed twice against dd H_2O before being finally dialyzed against KPi buffer (100 mM) overnight. The reconstituted ZnPP/apoMb (ZnMb) solution was first filtered with a cellulose membrane (0.2 μm) before being purified on a column (Sephadex G-25) pre-equilibrated with KPi buffer (100 mM, pH 6.8). The reconstituted ZnMb was eluted with the same buffer at 4 °C following the standard procedure. The desalted ZnMb solution was collected and stored at −20 °C for subsequent experiments.

2.3. Preparation of Eosin-Modified ZnMb

ZnMb was modified with eosin-5-isothiocyanate (Eosin) following the modified method of Zahavy et al.[30] Eosin reacts with amino and sulfhydryl groups on proteins to form a covalent bond according to these reactions:

Eosin-N=C=S + H_2N-protein → Eosin-NH-CS-protein

Eosin-N=C=S + HS-protein → Eosin-NH-CS-S-protein
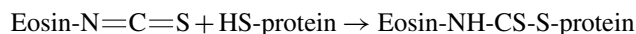
To prepare the concentrated solution (1 mg ml^{-1}) Eosin was first dissolved in phosphate buffer (0.1 M, pH 8). The freshly prepared ZnMb was first adjusted to pH 7.5 before adding the prepared eosin reagent. The molar ratio of protein:eosin was 1:3.5. Following the addition of eosin reagent, the solution was stirred for 20 h at 4 °C in the dark. The resulting solution was dialyzed twice (each dialysis was conducted for 3 h) against KPi buffer (1 L, pH 8). The eosin-modified ZnPP-Mb (EoZnMb) solution was purified through gel filtration on a column (Sephadex G-10, 2 × 5 cm), using KPi buffer (10 mM, pH 8) as eluent. The EoZnMb fraction was identified spectrometrically (wavelength 524 nm). The modification efficiency was calculated assuming an absorption coefficient of Eosin $\varepsilon = 83,000$ M^{-1} cm^{-1}. The modification efficiency of eosin to protein was observed between 1:1 and 2:1.

2.4. Protein Immobilization on TiO_2 Films

The factors that let redox proteins adsorb on a TiO_2 film are an electrostatic interaction between protein and film and a covalent binding between a cationic site on a metal surface (Ti) and oxygen of the carboxylate group.[29] The isoelectric point of TiO_2 has been shown to be in a region 6.1–6.3; the surface charge of TiO_2 film became negative when the pH was adjusted above 6.3. As the isoelectric point of Mb was 7.2, the pH of the buffer solution was adjusted to 7, so that the protein surface was positively charged while the TiO_2 surface was negatively charged. Mb, ZnMb, and EoZnMb protein samples (20 μL, 0.1 mM) were individually dropped onto TiO_2 films and incubated at 4 °C for four days. After protein adsorption, the TiO_2 films were rinsed with KPi buffer

(10 mM, pH 7.0) to remove the non-immobilized protein. The protein-immobilized TiO_2 films were dried with N_2 and subsequently subjected to spectral and photovoltaic measurements.

2.5. Steady-State and Temporally Resolved Spectral Measurements

The steady-state absorption spectra were recorded with a standard spectrometer (Cary 50, Varian); emission spectra were measured with a fluorescence spectrometer (Hitachi F-7000). The picosecond time-resolved spectra and anisotropy were measured with a time-correlated single-photon counting system (TCSPC, Fluo-Time 2000, PicoQuant) excited with a pulsed LED head (PLS-8-2-188, PicoQuant), coupled with a laser-diode driver (PDL-800B, PicoQuant). The FWHM of the excitation pulse was ∼750 ps; wavelength 510 nm was selected with an interference filter.

2.6. Photovoltaic Measurements

The performance of a DSSC device was examined through measurement of an I–V curve with a solar simulator (AM 1.5, Newport-Oriel 91160). The solar simulator uses filters and other optical components to mimic a solar radiation with an air mass 1.5 spectrum; the output intensity is evenly distributed to illuminate a large area. When the device was irradiated with the solar simulator, the source meter (Keithley 2400, computer-controlled) sent a voltage V to the device; photocurrent I was read at each step controlled with a computer via a GPIB interface. The solar simulator was calibrated with a Si-based reference cell (S1133, Hamamatsu) and an IR-cut filter (KG5) to correct the spectral mismatch of the lamp.[36] The actively illuminated area was 0.16 cm^2 for all measurements.

3. RESULTS AND DISCUSSION

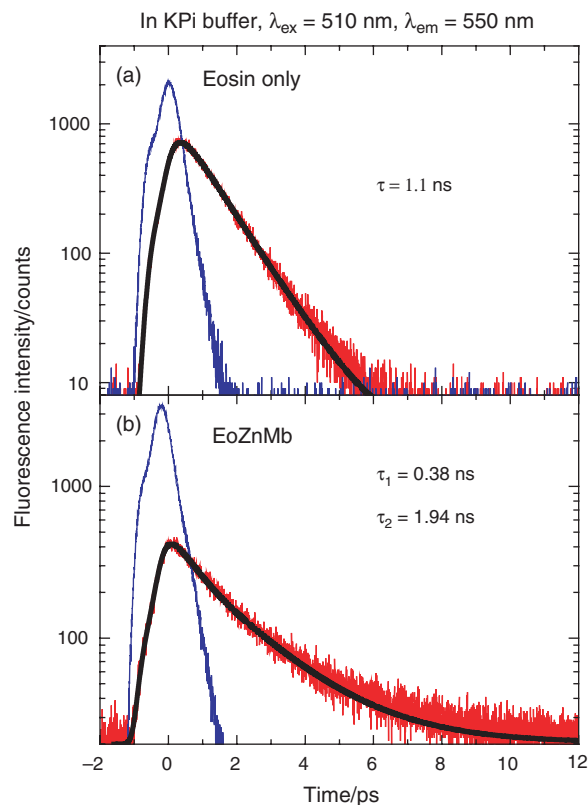### 3.1. Steady-State and Time-Resolved Spectral Measurements

Figure 1 shows the steady-state absorption and fluorescence spectra of (a) Mb, (b) ZnMb, (c) EoZnMb, and (d) Eosin in KPi tris-buffer solution. In Figure 1(a), the absorption spectrum of Mb features a broad line at ∼410 nm, which originated from the Soret band of the heme (iron-containing porphyrin) prosthetic group in the center.[27] For ZnMb (Fig. 1(b)), the absorption spectrum is consistent with our previous result,[37] in which the maxima at 428, 555 and 595 nm are attributed to B(0,0), Q(1,0) and Q(0,0) bands of ZnPP, respectively; the emission maxima are assigned as Q(0,0) and Q(0,1) at 600 and 650 nm, respectively. For EoZnMb (Fig. 1(c)), both ZnPP and Eosin contribute to the absorption patterns. Relative to spectrum of Eosin in a KPI buffer, the
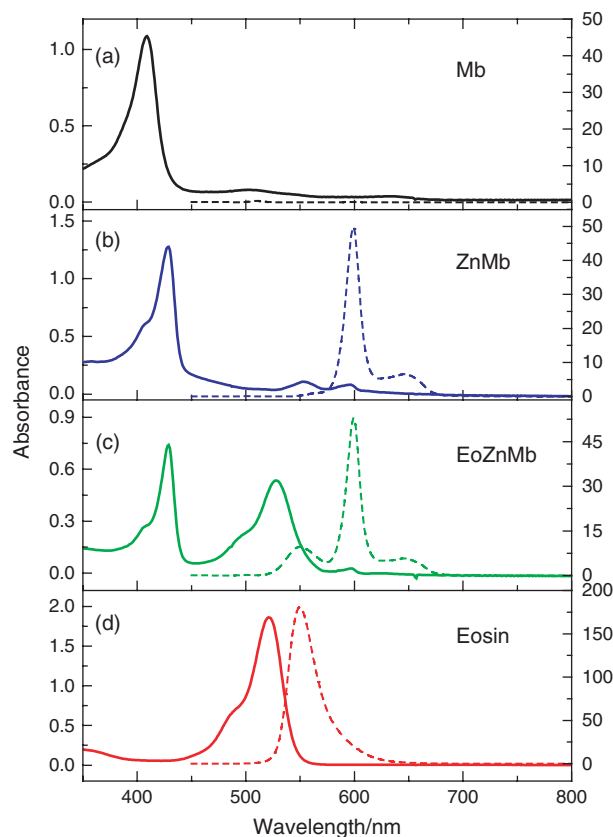
Fig. 1. Steady-state spectra of (a) Mb, (b) ZnMB, (c) EoZnMb and (d) Eosin in KPi buffer with concentrations of all compounds fixed at 10 μM. The absorption and emission spectra are shown as solid and dashed curves, respectively (excitation wavelength 428 nm for Mb, ZnMb, and EoZnMb, but 510 nm for Eosin).

In KPi buffer, $\lambda_{ex} = 510$ nm, $\lambda_{em} = 550$ nm


Fig. 2. Picosecond time-resolved fluorescence decays of (a) Eosin and (b) EoZnMb in KPi buffer; excitation and probe wavelengths fixed at 510 and 550 nm, respectively. The raw data and fitted curves are shown as red and black traces, respectively; the instrument response functions (IRF) are shown as blue traces. The fluorescence decays were deconvoluted with the IRF and the corresponding time coefficients as indicated.

absorption of Eosin in EoZnMb is slightly red-shifted (521 vs. 528 nm) because of the formation of chemical binding between Eosin and Mb moieties. The emission spectrum of EoZnMb features the characteristic emissions of both ZnPP and Eosin, indicating no efficient occurrence of energy transfer between those two chromophores.

Figures 2(a) and (b) show the picosecond fluorescent decays of Eosin and EoZnMb in buffer, respectively. To avoid the interference of ZnPP, we fixed the excitation wavelength at 510 nm and set the probe wavelength at 550 nm, which corresponds to the emission maximum of Eosin. After deconvolution with the instrument response function (shown as blue traces), we determined the fluorescence lifetime of free Eosin to be 1.1 ns, consistent with a typical period for $S_1 \rightarrow T_1$ intersystem crossing (ISC) of Eosin reported in the literature.[38] For EoZnMb (Fig. 2(b)), the fluorescence transient exhibits a bi-exponential decay with two time coefficients determined to be 0.38 and 1.94 ns. The rapid component of EoZnMb (0.38 ns), absent from free Eosin, is assigned to result from energy transfer between Eosin and the amino acid of the protein. The slow component of EoZnMb decayed much more slowly than that of free Eosin (1.94 ns vs. 1.1 ns); we expect

that the Eosin moiety was located in a rather hydrophobic environment relative to free Eosin in buffer. Moreover, the rigidity of Eosin bound to protein might be considered to be a factor yielding a greater lifetime. To provide further spectral evidence to prove that Eosin was bound to ZnMb in EoZnMb as indicated in Scheme 1, we measured the temporally resolved fluorescence anisotropy of free Eosin and EoZnMb with the same excitation and probe wavelengths.

The basic principle of fluorescence anisotropy is described elsewhere.[39] The fluorescence anisotropy at time t, $r(t)$, is expressible as

$$r(t) = \frac{I_{VV}(t) - G \cdot I_{VH}(t)}{I_{VV}(t) + 2G \cdot I_{VH}(t)} \quad (1)$$

in which $I_{VV}(t)$ and $I_{VH}(t)$ represent fluorescence transients for excitation with vertically polarized light and probed with vertically and horizontally polarized light, respectively. Because the efficiency of vertically and horizontally polarized light through the monochromator differed, we corrected for the excitation at the horizontal polarization and the probe at vertical (I_{HV}) and horizontal (I_{HH}) polarizations, which yields a G factor defined by
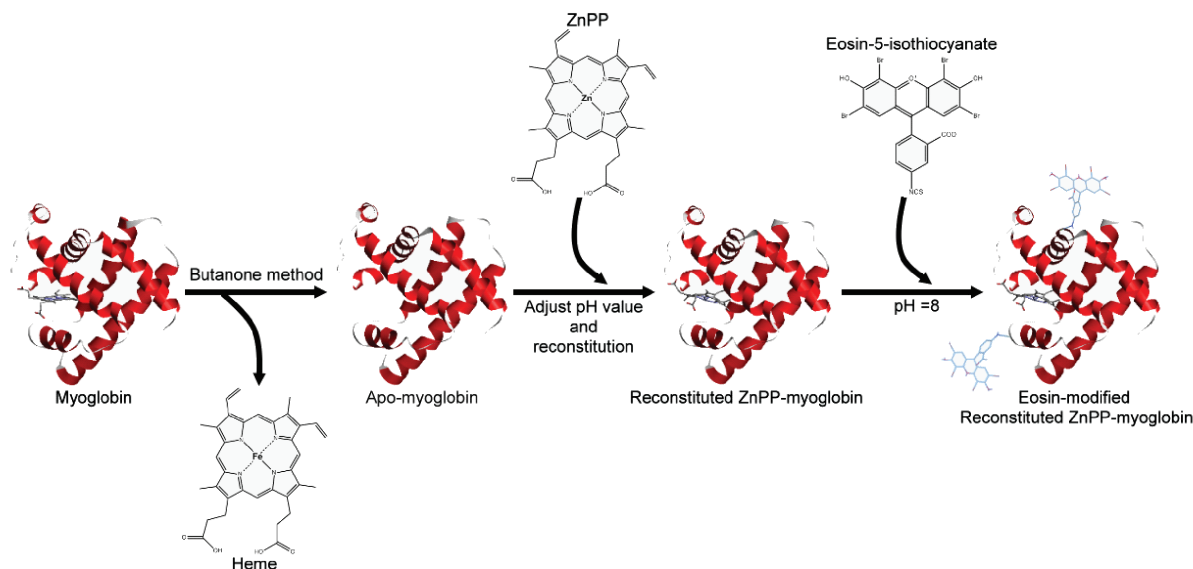
Scheme 1.   Reaction to form reconstituted ZnPP-myoglobin (ZnMb) and Eosin-modified reconstituted ZnPP-myoglobin (EoZnMb).

the ratio I_{HV}/I_{HH}. Figure 3 shows the corresponding fluorescence transients of EoZnMb; the time-dependent fluorescence anisotropies of Eosin and EoZnMb are shown in the inset for comparison. For Eosin alone, the time-resolved fluorescence anisotropy was fitted with a single exponential decay function with a time coefficient less than 0.8 ns, limited by the broad instrument response function (FWHM = 0.75 ns), but the time-resolved fluorescence anisotropy of EoZnMb persists into the ns time scale. These results indicate that the rotational motion of the Eosin moiety was suppressed in EoZnMb; Eosin seems to have been firmly bound to ZnMb as proposed in Scheme 1.
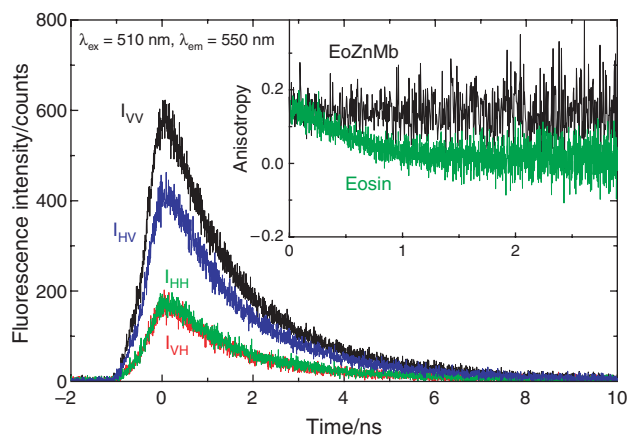

Fig. 3.   Fluorescence transient components recorded at various polarizations to construct the time-dependent anisotropy of EoZnMb in KPi buffer. The inset shows a comparison of the constructed fluorescence anisotropies of Eosin and EoZnMb in KPi buffer. For Eosin (green trace), the decay of the anisotropy was instrument-limited; for EoZnMb (black trace), no decay was observed within 0–3 ns.

3.2. Fabrication of a Bio-Sensitized Solar Cell and Photovoltaic Measurements

With Mb, ZnMb and EoZnMb as sensitizers, we fabricated the corresponding BSSC devices according to a standard procedure of DSSC.[40, 41] TiO$_2$ nanoparticles ($\sim$20 nm) prepared with a sol–gel method[41] were screen-printed on a F-doped SnO$_2$ (FTO) glass. The area of TiO$_2$ was fixed at 0.16 cm^2 (4 mm $\times$ 4 mm). The sensitization of the working electrode was achieved on soaking the TiO$_2$ films in buffer solutions containing the proteins for about four days. Because the adsorption of protein on TiO$_2$ was sensitive to the pH of the buffer solution, the pH was kept at 7. To avoid degradation of the bio-sensitizers, we controlled the temperature at 4 °C. After sensitization, the electrodes were washed with buffer solution to remove the unsensitized protein molecules. The sensitized TiO$_2$ films were assembled with a Pt-coated counter electrode; the space between the two electrodes was filled with electrolyte 1376,[42] composed of M-methyl-N-butyl imidazolium iodide (0.6 M), diiodine (0.05 M), LiI (0.05 M), and *tert*-butylpyridine (0.5 M) in a mixture of valeronitirile and acetonitrile (50:50 v/v).

Figures 4(a, b, and c) show absorption spectra of Mb, ZnMb and EoZnMb-sensitized TiO$_2$ films (solid curves) and the corresponding absorption spectra in buffer solutions (dashed curves). For Mb-sensitized TiO$_2$ film, apart from the scattering caused by TiO$_2$ nanoparticles, the absorption spectrum resembles that in buffer solution. The result indicates that the aggregation and the solvation of the Heme porphyrin were suppressed by the surrounding apomyoglobin moiety. In contrast, the hypsochromic shift of the Soret bands in ZnMB- and EoZnMb-sensitized TiO$_2$ films indicate that ZnPP might reside in a relatively hydrophobic site.
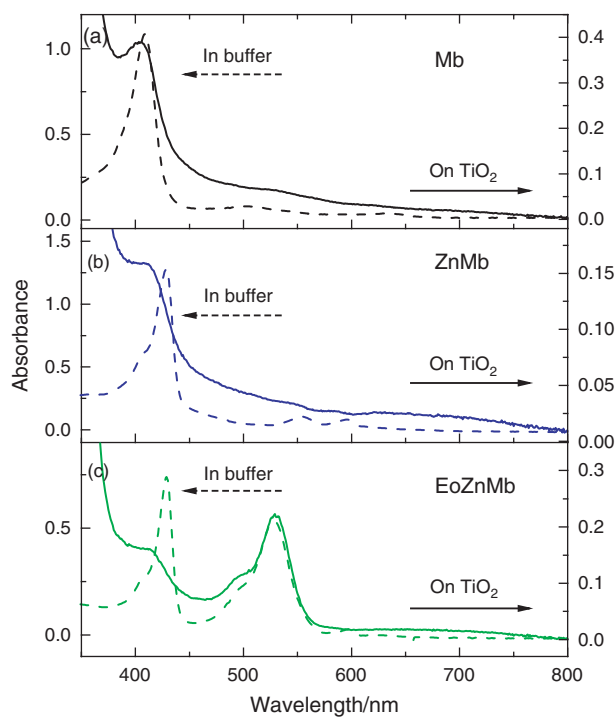
Fig. 4. Absorption spectra of (a) Mb, (b) ZnMb and (c) EoZnMb immobilized on TiO_2 films (solid curves) and in KPi buffer (dashed curves).

The efficiency (η) of conversion of light to electricity is

$$\eta = \frac{P_{mp}}{P_{in}} = \frac{I_{mp}V_{mp}}{P_{in}} = \frac{I_{SC}V_{OC}FF}{P_{in}} \qquad (2)$$

in which P_{in} is the input radiation power of the solar simulator (100 mW cm^{-2}), P_{mp} is the maximum output power ($=I_{mp} \times V_{mp}$), and the fill factor (FF) is defined as

$$FF = \frac{I_{mp}V_{mp}}{I_{SC}V_{OC}} \qquad (3)$$

in which I_{SC} (mA) is the current measured at short circuit and V_{OC} (V) is the voltage measured at open circuit. The measured photovoltaic parameters are summarized in Table I; the corresponding I–V curves are demonstrated in Figure 5. For comparison, the I–V curves of blank TiO_2 films before sensitization were measured as references. For ZnMb, I_{SC} increased from 43 μA cm^{-2} for a blank TiO_2 film to 55 μA cm^{-2} for a sensitized TiO_2 film, with V_{OC} concurrently increasing significantly from

Table I. Photovoltaic parameters of bio-sensitized solar cells under illumination (AM 1.5, power 100 mW cm^{-2}) with active area 0.16 cm^2. For comparison, the values between parentheses are the cell performances of blank TiO_2 films measured before sensitization.

| Sensitizers	J_{SC}/μA cm^{-2}	V_{OC}/V	FF	η (%)
Mb	13 (26)	0.24 (0.16)	0.40 (0.35)	0.001 (0.001)
ZnMb	55 (43)	0.47 (0.10)	0.58 (0.31)	0.015 (0.001)
EoZnMb	64 (34)	0.45 (0.15)	0.51 (0.34)	0.015 (0.002)
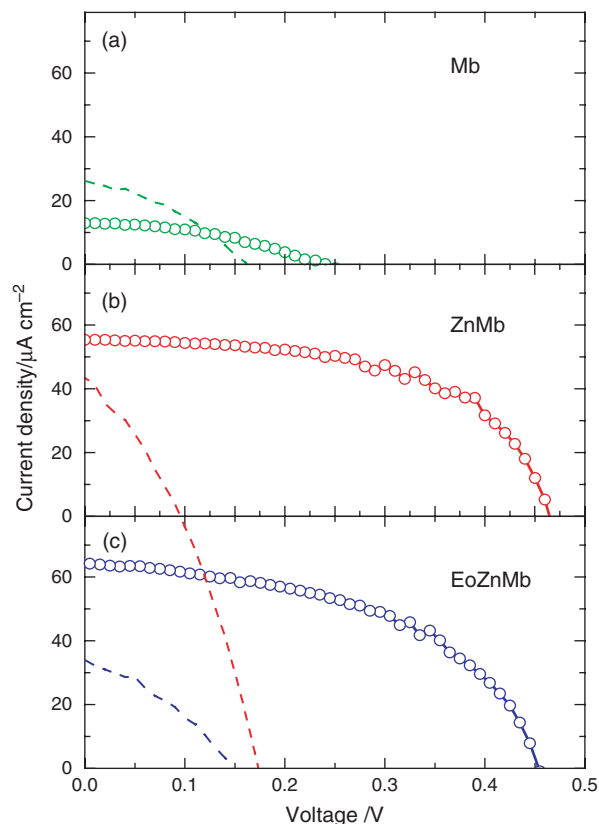
Fig. 5. Photovoltaic characteristics of (a) Mb-, (b) ZnMb- and (c) EoZnMb-sensitized solar cells, performed under illumination at AM 1.5, and 100 mW cm^{-2}. For comparison, the IV-characteristics of individual blank TiO_2 films before sensitization are shown as dashed curves.

0.1 V to 0.47 V and FF increasing from 0.31 to 0.58. The overall efficiency of power conversion was effectively increased from 0.001% for a blank TiO_2 film to 0.015% for a ZnMb-sensitized film. These substantial increases of both I_{SC} and V_{OC} indicate that the electrons in the excited state of ZnPP are efficiently injected into the conduction band of TiO_2 through the surrounding apomyoglobin. For EoZnMb, the increment of the current density was even more substantial: I_{SC} increased from 34 μA cm^{-2} for a blank TiO_2 film to 64 μA cm^{-2} for an EoZnMb-sensitized TiO_2 film, which is more than twice that for the ZnMb-sensitized film. As the absorbances of the Soret bands of ZnPP were similar in these two films ($\sim$0.16), the increase density of photo-induced current reflected the contribution of the Eosin moiety, but the filling factor of the BSSC device made of the EoZnMb-sensitized film was not great ($FF = 0.51$), which yields an overall efficiency of power conversion the same as that of the ZnMb-sensitized film ($\eta = 0.015\%$).

In contrast, I_{SC} decreased from 26 μA cm^{-2} for the blank TiO_2 film to 13 μA cm^{-2} for the Mb-sensitized TiO_2 film even though its V_{OC} increased from 0.16 V to 0.24 V. As the decreased I_{SC} was balanced by the increases of both V_{OC} and FF, the overall efficiency of power conversion
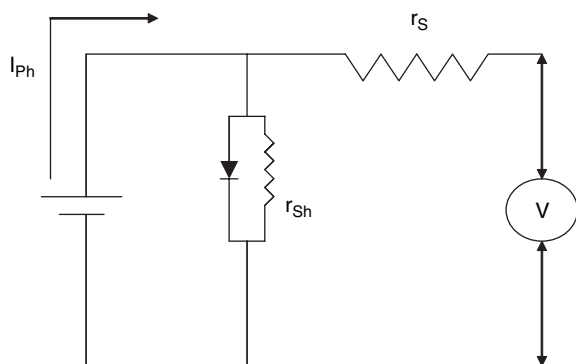
Fig. 6. Schematic representation of an equivalent circuit for a BSSC device.

of the BSSC device made from the Mb-sensitized TiO_2 film was essentially the same as for the unsensitized TiO_2 film ($\eta \sim 0.001$). The reason for the poor cell performance of Mb-sensitized TiO_2 film is as follows. The absorption spectrum of Mb in the steady state (Fig. 4(a)) indicates that the heme group in Mb exists in an oxidized form Fe(III).[27] The generation of conduction-band electrons in the TiO_2 film has been found to reduce Fe(III) of the heme group to Fe(II).[27] This reduction can be considered to be an extra channel of current loss, such that we observed a significant decrease of photocurrent for the Mb-sensitized TiO_2 film.

A simple way to analyze the cell performance of a BSSC device involves use of an equivalent circuit. Figure 6 shows the equivalent circuit for a solar cell; the slopes of the I–V curve calculated at $I = 0$ and $V = 0$ yield inverse values of a series resistance r_S (bulk resistivity of the materials or contact resistance) and the shunt resistance r_{Sh} (current leakage), respectively.[43–46] In Figure 5, the slopes at $I = 0$ are similar in all films, indicating that they all have similar series resistances, but at $V = 0$ the slopes of the protein-sensitized TiO_2 films were significantly smaller than those of the blank films. This result indicates that the increased shunt resistances were due to adsorption of protein molecules on the TiO_2 surface so as to decrease appreciably the dark current. That increased shunt resistance signifies that the current leakage or the electron transfer from the TiO_2 film to the electrolyte was substantially decreased, which effectively raises the Fermi level of the TiO_2 film. Because V_{OC} is determined by the difference between the Fermi level of TiO_2 and the reduction potential of the electrolyte,[5] we observed the V_{OC} values of all protein-sensitized TiO_2 films to become significantly increased, even for the Mb-sensitized TiO_2 film. The observed enhanced performances in both ZnMb and EoZnMb–sensitized SC were due not only to the effect of light harvesting that increased I_{SC}, but also the significantly decreased leakage of current from TiO_2 to the electrolyte that results in increased shunt resistances of the device so as to increase both V_{OC} and *FF* in both BSSC.

4. CONCLUSION

We characterized three bio-sensitized solar cells (BSSCs) fabricated with myoglobin (Mb), reconstituted zinc protoporphyrin-apomyoglobin (ZnMb), and eosin-modified reconstituted zinc protoporphyrin-apomyoglobin (EoZnMb) as photosensitizers. The Mb-sensitized SC exhibits a poor cell performance because of the internal electron transfer that reduces Fe(III) to Fe(II) so that a small photocurrent is observed. For both ZnMb- and EoZnMb-sensitized SCs, the efficiencies of power conversion were found to be enhanced ten times those of their unsensitized counterparts (blank TiO_2 SC), through efficient electron injection from the proteins to TiO_2 that improves the charge separation between TiO_2 and the sensitizer and decreased current leakage between TiO_2 and the electrolyte. The present work provides the first practical example of BSSC devices made with artificial proteins as potential photosensitizers. Relative to a typical DSSC, the power conversion efficiency of a BSSC was still too small because the extent of immobilization of the proteins on the surface of TiO_2 was too slight. Work is in progress to improve the cell performance of BSSC under investigation by increasing the adsorption of the proteins on TiO_2 films and by seeking more appropriate bio-related electrolytes.

References and Notes

1. M. Grätzel, *Chem. Lett.* 34, 8 (**2005**).
2. S. C. Doney and D. S. Schimel, *Annu. Rev. Environ. Resour.* 32, 31 (**2007**).
3. S.-N. Chen, S. K. Deb, and H. Witzke, U.S. Patent 4080488 (**1978**).
4. B. O'Regan and M. Grätzel, *Nature* 353, 737 (**1991**).
5. M. Grätzel, *Inorg. Chem.* 44, 6841 (**2005**).
6. M. K. Nazeeruddin, R. Humphry-Baker, M. Grätzel, and B. A. Murrer, *Chem. Commun.* 719 (**1998**).
7. J. He, A. Hagfeldt, and S.-E. Lindquist, *Langmuir* 17, 2743 (**2001**).
8. G. Ramakrishna and H. N. Ghosh, *J. Phys. Chem. B* 105, 7000 (**2001**).
9. G. Ramakrishna, A. Das, and H. N. Ghosh, *Langmuir* 20, 1430 (**2004**).
10. H. N. Ghosh, *J. Phys. Chem. B* 103, 10382 (**1999**).
11. K. Hara, T. Sato, R. Katoh, A. Furube, Y. Ohga, A. Shinpo, S. Suga, K. Sayama, H. Sugihara, and H. Arakawa, *J. Phys. Chem. B* 107, 597 (**2003**).
12. K. Wongcharee, V. Meeyoo, and S. Chavadej, *Sol. Energy Mater. Sol. Cells* 91, 566 (**2007**).
13. T. Yagishita, S. S. Yama, K. Tsukahara, and T. Ogi, *J. Biosci. Bioeng.* 88, 210 (**1999**).
14. D. Das, P. J. Kiley, M. Segal, J. Norville, A. A. Yu, L. Wang, S. A. Trammell, L. E. Reddick, R. Kumar, F. Stellacci, N. Lebedev, J. Schnur, B. D. Bruce, S. Zhang, and M. Baldo, *Nano. Lett.* 4, 1079 (**2004**).

RESEARCH ARTICLE

15. D. Ho, B. Chu, H. Lee, E. K. Brooks, K. Kuo, and C. D. Montemagno, *Nanotechnology* 16, 3120 (**2005**).

16. T. Miyasaka, K. Koyama, and I. Itoh, *Science* 255, 342 (**1992**).

17. V. Renugopalakrishnan, A. Mershin, T. Velmurugan, S. Filipek, M. Kolinski, E. Padrós, C. S. Verma, M. Ortiz-Lombardía, and S. Ramakrishna, *Nat. Nanotechnol.* (**2008**), in press.

18. S. Tsujimura, A. Wadano, K. Kano, and T. Ikeda, *Enz. Microb. Technol.* 29, 225 (**2001**).

19. K. B. Lam, E. A. Johnson, M. Chiao, and L. Lin, *J. Microelectromech. Syst.* 15, 1243 (**2006**).

20. Y. Lu, M. Yuan, Y. Liu, B. Tu, C. Xu, B. Liu, D. Zhao, and J. Kong, *Langmuir* 21, 4071 (**2005**).

21. Q. Wang, W. M. Campbell, E. E. Bonfantani, K. W. Jolley, D. L. Officer, P. J. Walsh, K. Gordon, R. Humphry-Baker, M. K. Nazeeruddin, and M. Grätzel, *J. Phys. Chem. B* 109, 15397 (**2005**).

22. P. Y. Reddy, L. Giribabu, C. Lyness, H. J. Snaith, C. Vijaykumar, M. Chandrasekharam, M. Lakshmikantam, J.-H. Yum, K. Kalyanasundaram, M. Grätzel, and M. K. Nazeeruddin, *Angew. Chem. Int. Ed.* 46, 373 (**2007**).

23. J. Rochford, D. Chu, A. Hagfeldt, and E. Galopini, *J. Am. Chem. Soc.* 129, 4655 (**2007**).

24. S. Gadde, D.-M. S. Islam, C. A. Wijesinghe, N. K. Subbaiyan, M. E. Zandler, Y. Araki, O. Ito, and F. D'Souza, *J. Phys. Chem. C* 111, 12500 (**2007**).

25. W. M. Campbell, K. W. Jolley, P. Wagner, K. Wagner, P. J. Walsh, K. C. Gordon, L. Schmidt-Mende, M. K. Nazeeruddin, Q. Wang, M. Grätzel, and D. L. Officer, *J. Phys. Chem. C* 111, 11760 (**2007**).

26. L. Luo, C.-H. Chang, Y.-C. Chen, T.-K. Wu, and E. W.-G. Diau, *J. Phys. Chem. B* 111, 7656 (**2007**).

27. E. Topoglidis, T. Lutz, R. L. Willis, C. J. Barnett, A. E. G. Cass, and J. R. Durrant, *Faraday Discuss.* 116, 36 (**2000**).

28. E. Topoglidis, C. J. Campbell, A. E. G. Cass, and J. R. Durrant, *Electroanalysis* 18, 882 (**2006**).

29. E. Topoglidis, E. Palomares, Y. Astuti, A. Green, C. J. Campbell, and J. R. Durrant, *Electroanalysis* 17, 1035 (**2005**).

30. E. Zahavy and I. Willner, *J. Am. Chem. Soc.* 118, 12499 (**1996**).

31. W.-P. Tai and K. Inoue, *Mat. Lett.* 57, 1508 (**2003**).

32. F. W. Teale, *Biochim. Biophys. Acta* 35, 543 (**1959**).

33. I. Hamachi, S. Tanaka, and S. Shinkai, *J. Am. Chem. Soc.* 115, 10458 (**1993**).

34. Y.-Z. Hu, S. Tsukiji, S. Shinkai, S. Oishi, and I. Hamachi, *J. Am. Chem. Soc.* 122, 241 (**2000**).

35. Y.-Z. Hu, H. Takashima, S. Tsukiji, S. Shinkai, T. Nagamune, S. Oishi, and I. Hamachi, *Chem. Eur. J.* 6, 1907 (**2000**).

36. S. Ito, H. Matsui, K.-I. Okada, S.-I. Kusano, T. Kitamura, Y. Wada, and S. Yanagida, *Sol. Energy Mater. Sol. Cells* 82, 421 (**2004**).

37. L. Luo, C.-H. Chang, Y.-C. Chen, T.-K. Wu, and E. W.-G. Diau, *J. Phys. Chem. B* 111, 7656 (**2007**).

38. G. R. Fleming, A. W. E. Kinght, J. M. Morris, R. J. S. Morrison, and G. W. Robinson, *J. Am. Chem. Soc.* 99, 4306 (**1977**).

39. V. Bernard, Molecular Fluorescence: Principles and Applications, Wiley-VCH, Weinheim, Germany (**2002**).

40. S. Ito, P. Chen, P. Comte, M. K. Nazeeruddin, P. Liska, P. T. Pe'chy, and M. Grätzel, *Prog. Photovolt: Res. Appl.* 15, 603 (**2007**).

41. P. Wang, S. M. Zakeeruddin, P. Comte, R. Charvet, R. Humphry-Baker, and M. Grätzel, *J. Phys. Chem. B* 107, 14336 (**2003**).

42. M. K. Nazeeruddin, R. Humphry-Baker, D. L. Officer, W. M. Campbell, A. K. Burrell, and M. Grätzel, *Langmuir* 20, 6514 (**2004**).

43. A. Moliton and J.-M. Nunzi, *Polym. Int.* 55, 583 (**2006**).

44. M. Muraysma and T. Mori, *Thin Solid Films* 509, 123 (**2006**).

45. L. Han, N. Koide, Y. Chiba, and T. Mitate, *Appl. Phys. Lett.* 84, 2433 (**2004**).

46. L. Han, N. Koide, Y. Chiba, A. Islam, and T. Mitate, *C. R. Chimie* 9, 645 (**2006**).